

# ASSESSMENT OF MACH STEM PRESSURES: COMPARISON OF EXPERIMENTS WITH ENGINEERING AND EULERIAN MODELS

Len Schwer

Schwer Engineering & Consulting Services

## 1 Introduction

Laboratory scale tests conducted by Kisters and Kuder (2012) provide reflected pressure histories for a 1kg TNT charge detonated at 0.32m above a rigid surface. The pressure histories are measured 1m from the charge using a vertical array of pressure transducers to infer the height of the Mach Stem at this range. Two such vertical arrays, each with 9 pressure transducers at varying heights above the surface, were used, and the test was repeated three times. Four additional configurations with heights-of-burst (HOB) varying from 0.1 to 0.32m and standoff ranges of 0.9 to 1.2m were conducted, but not reported in the present reference. Examination of the measured wave forms allowed Kisters and Kuder to estimate the height of the Mach Stem, a.k.a. triple point, to within 60mm (vertical gauge spacing).

The pressure histories from the vertical array measurements provide an opportunity to assess the accuracy of the LS-DYNA air blast engineering model referred to as `LOAD_BLAST_ENHANCED`, and results from simulations using the LS-DYNA Eulerian solver usually referred to as Multi-Material Lagrangian Eulerian (MM-ALE). In addition to comparisons of maximum pressure, and time-of-arrival (TOA), the time integrated pressure histories provide maximum impulses for comparison.

## 2 Brief Description of the Laboratory Experiments

As described by Kisters and Kuder (2012), the laboratory test configuration consists of a 2m square steel plate placed over a sand pit in the floor of the laboratory, see Figure 1. The 1kg spherical TNT charge was placed at the center of the steel plate and supported by a Styrofoam block. The pressures reported by Kisters and Kuder are from pressure sensors in vertical arrays located 1m from the charge at opposite corners of the steel plate. Each vertical array contains 9 pressure transducers spaced 60mm apart with the lowest sensor 80mm above the steel plate, i.e. 80, 140, 200, 260, 320, 380, 500, and 560mm. The present Kisters and Kuder reference does not provide data from the other gauges shown in Figure 1.

## 3 Measured Pressure Histories

Pressure histories at eight of the nine pressure gauges are shown in Figure 2. As discussed by Kisters and Kuder, below the triple point, i.e. below 260mm in this configuration, there is only a single pressure peak at the TOA for the Mach Stem. Above the triple point, two distinct pressure peaks are observed, the first corresponding to the arrival of the incident wave and the second the arrival of the reflect wave; reflected from the steel plate.



Figure 1 Laboratory test and instrumentation configuration (left) and vertical pressure array right; Figure 3 in Kisters and Kuder (2012).

The pressure wave forms are annotated by Kisters and Kuder to indicate the TOA for an incident wave in the absence of a reflective surface, i.e. free air burst TOA, by the nearly vertical dash line (color blue) with the earliest arrival time. Note the minimum range to a pressure gauge occurs at a height of 320mm, i.e. the same as the HOB, and provides the minimum TOA for a free air burst. The other dashed line (color green), at nearly a 45 degree angle, indicates the TOA of the reflected wave.

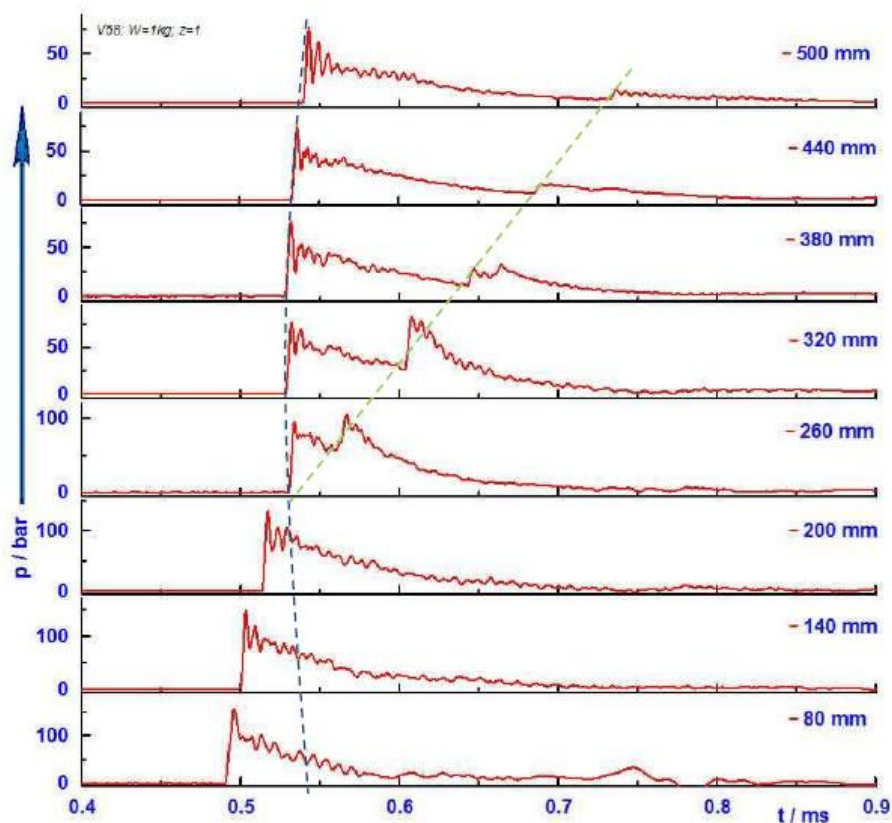


Figure 2 Measured pressure histories for 1kg spherical TNT charge at 0.32m HOB at a standoff of 1m; Figure 4 in Kisters and Kuder (2012).

## 4 Engineering Model Results Comparisons

Mach stem air blast results from two engineering models are presented in this section.

The LS-DYNA keyword `LOAD_BLAST_ENHANCED` provides an engineering (empirical) model of air blast. In addition to free air blast, identical to the `ConWep` functionality, `LOAD_BLAST_ENHANCED` optionally provides pressure histories for a height-of-burst simulation. *Note: the `LOAD_BLAST_ENHANCED` results in this manuscript reflect improvements made to height-of-burst portion of `LOAD_BLAST_ENHANCED` included in R80022 (27 Feb 2013) and more recent versions.*

The CAB engineering model is from the US Army Engineering Research and Development Center (ERDC): CAB (Close-in Air Blast) with air blast capabilities beyond those offered by `ConWep` (Conventional Weapons). CAB is based on Eulerian simulations, using the SAGE code. CAB uses these Eulerian results in the form of “tabular source models,” i.e. interpolation of stored Eulerian results<sup>1</sup>.

The `LOAD_BLAST_ENHANCED` height-of-burst model is based on charts provided in UFC 3-340-02 (2008)<sup>2</sup>. In particular, Figures 2-7, 2-9, 2-10 and 2-13. The last of these figures, i.e. Figure 2-13, provides the height of the triple point as a function of scaled range. The parameterized scaled height-of-burst, i.e. the height of burst divided by the cube root of the explosive mass, for this chart is limited to values between 1 and 7 ft / lbf<sup>1/3</sup> (0.39 to 2.77 m / kg<sup>1/3</sup>). The present Kisters and Kuder scaled height of burst is 0.32 m / kg<sup>1/3</sup>, slightly less than the lower end provided by Figure 2-13. For this reason the `LOAD_BLAST_ENHANCED` algorithm issues a warning message “Mach stem calculation may be inaccurate.” The reader is advised that only the height of the triple point may be inaccurate in the present case, as the other two charts that use scaled height of burst, i.e. Figures 2-9 and 2-10, provide parameter values for ranges between 0.3 and 14.3 ft / lbf<sup>1/3</sup> (0.12 to 5.67 m / kg<sup>1/3</sup>), and thus are applicable to the present scaled height of burst.

For the present simulation of Kisters and Kuder (2012) results, both engineering models consist of the description of the charge, i.e. mass and location. For the `LOAD_BLAST_ENHANCED` model shell elements are placed at the gauge locations to record the reflected pressure. Details of the `LOAD_BLAST_ENHANCED` keyword input parameters are provided in an appendix. For the CAB model, a description of the gauge array is included via a specification of ‘target points’ to record the pressure histories. A screen capture of the CAB graphical user interface input is provided in an appendix.

Figure 3 shows the `LOAD_BLAST_ENHANCED` predicted triple point path as the narrow region between the red (Mach Stem) and blue (incident and reflected wave region). The Mach Stem is predicted to intersect the vertical gauge array near the 260mm gauge.

---

<sup>1</sup> Personal communication with Robert (Bob) Britt of ERDC, developer of BLASTX, January 2012

<sup>2</sup> This UFC supersedes ARMY TM 5-1300, dated November 1990.

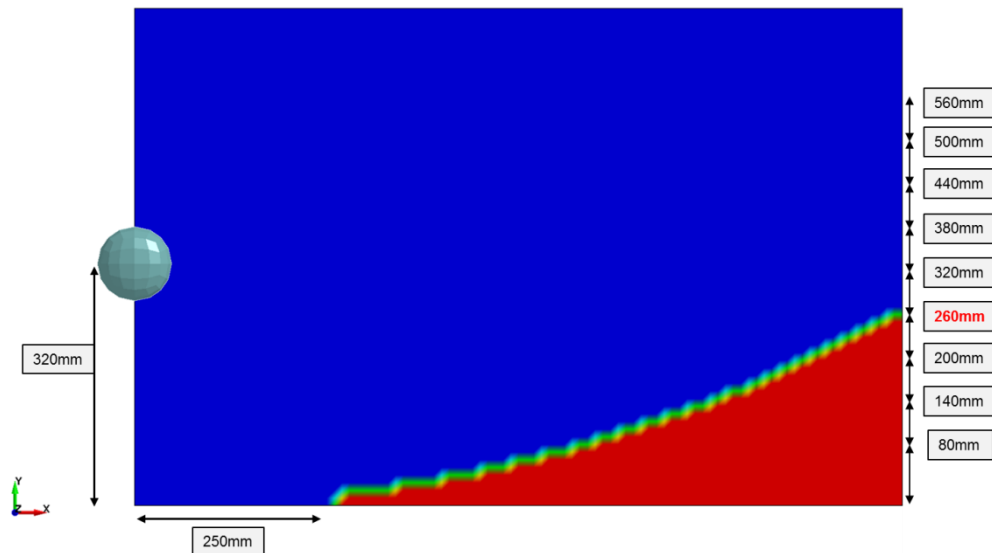


Figure 3 Illustration of *LOAD\_BLAST\_ENHANCED* predicted triple point path.

Figure 4 shows the *LOAD\_BLAST\_ENHANCED* pressure histories for the two gauges on either side of the Mach Stem triple point. The gauge at 260mm has a single pressure peak, indicating the pressure in the Mach Stem region. The gauge at 320mm has two distinct pressure peaks indicating the arrival of the incident wave, at about 0.52ms, and later the reflected wave arrival at about 0.56ms. Figure 5 is an illustration of the two gauge locations and the pressure waves that interact with each gauge.

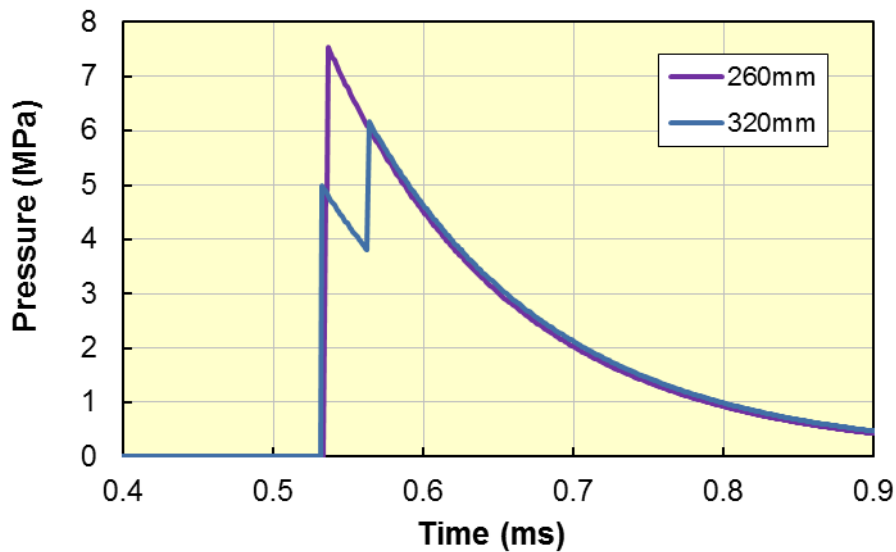


Figure 4 *LOAD\_BLAST\_ENHANCED* pressure histories near Mach Stem triple point.

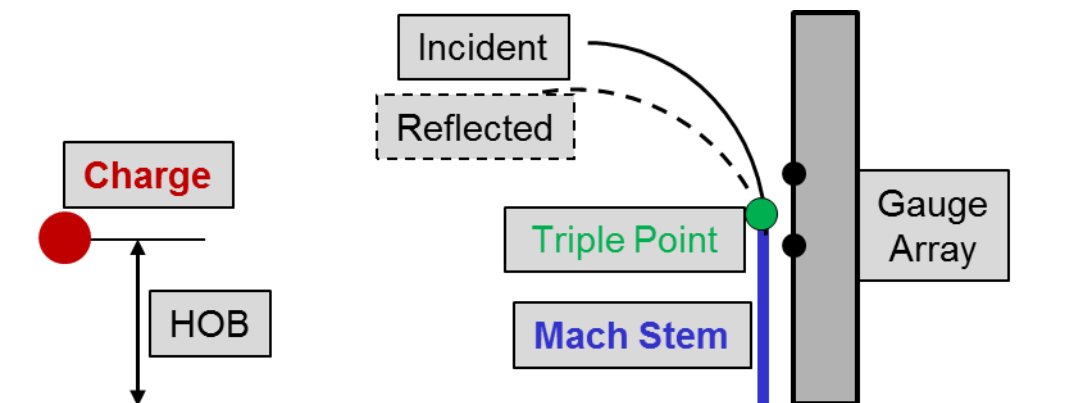


Figure 5 Illustration of Mach Stem (blue) and incident (solid black) and reflected (dashed black) waves interacting with gauges above and below the triple point.

Figure 6 shows a comparison of the pressure histories provided by Kisters and Kuder<sup>3</sup>, LS-DYNA's LOAD\_BLAST\_ENHANCED, and CAB at three gauge locations near the triple point. In the lower image, i.e. the gauge at 200mm, all three wave forms indicate the arrival of a single peak (maximum) pressure wave and imply this gauge is below the triple point. The CAB model predicts a slightly early arrival time compared to the data and the LOAD\_BLAST\_ENHANCED model predicts a later wave arrival. Both engineering models provide fairly good estimates of the maximum pressure cited by Kisters and Kuder of 9.75MPa: LOAD\_BLAST\_ENHANCED is about 10% low and CAB about 5% low; recall maximum pressures are notoriously difficult to measure, and predict numerically.

At the 260mm gauge location, middle image in Figure 6, the data shows a pressure history with two distinct peak pressures, implying a gauge location above the triple point as both the incident and reflected waves produce peak pressures. The LOAD\_BLAST\_ENHANCED and CAB results however, have only one pressure peak, again indicating a location below the triple point. The arrival of the LOAD\_BLAST\_ENHANCED incident (first) pressure peak corresponds almost exactly with the Kisters and Kuder data, but again the CAB wave arrives too early. The LOAD\_BLAST\_ENHANCED and CAB predicted maximum pressures provide good approximations of the Kisters and Kuder data.

The LOAD\_BLAST\_ENHANCED and CAB predictions provide two pressure peaks at the 320mm gauge location, implying a triple point height greater than observed by Kisters and Kuder. However, the magnitude and arrival times for both wave forms are quite good for the CAB prediction at this gauge height. LOAD\_BLAST\_ENHANCED predicts an early arrival of the reflected wave at about 0.56ms compared to the Kisters and Kuder data reflected wave at about 0.60ms.

Detailed comparisons of maximum pressures, impulses, and times-of-arrival are provided in the following subsections.

<sup>3</sup> The Kisters and Kuder pressure histories were crudely hand digitized from the wave forms shown previously in Figure 2.

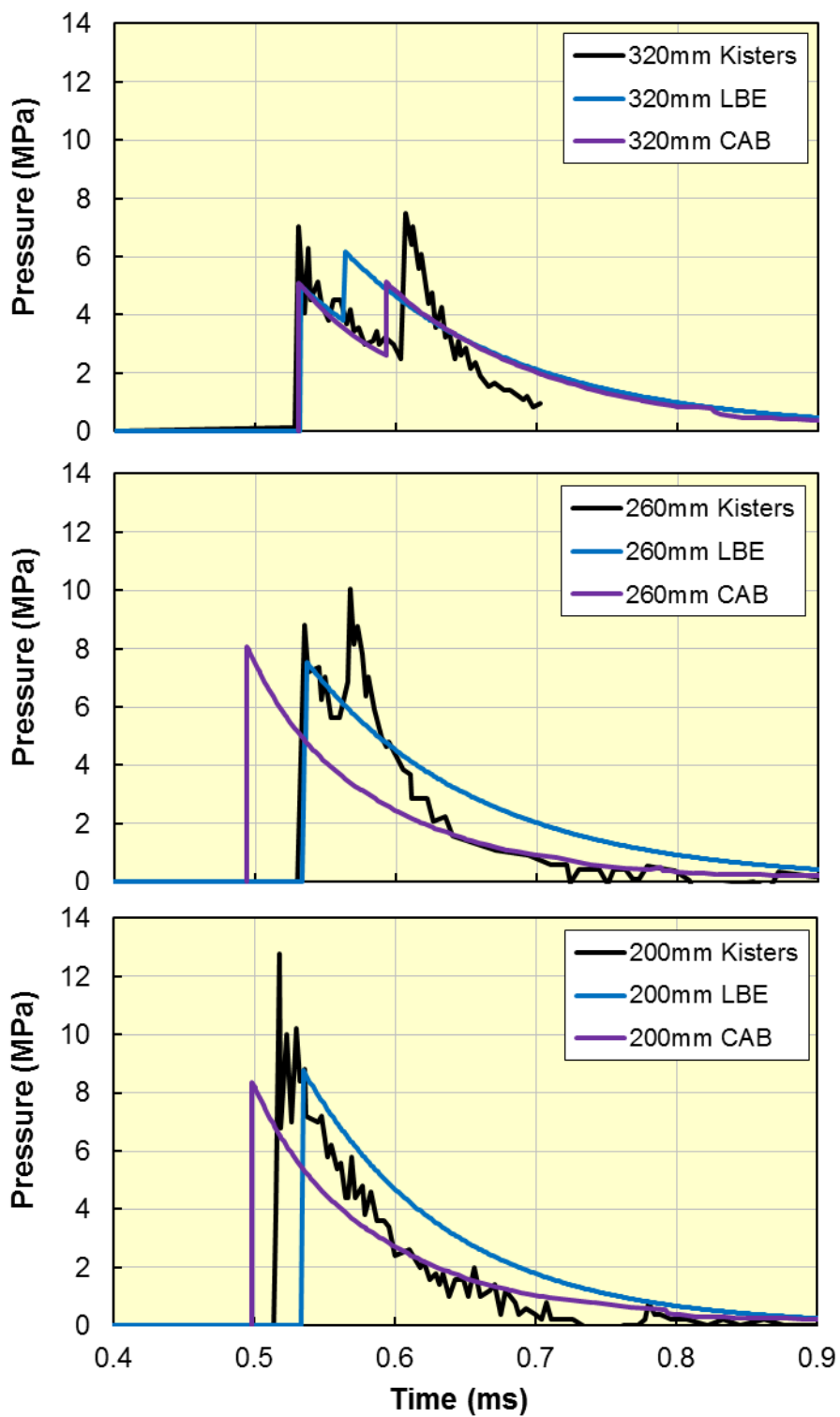


Figure 6 Comparison of pressure histories at three gauge locations near the triple point.

#### 4.1 Time-of-Arrival

Figure 7<sup>4</sup> presents a graphical comparison of the times-of-arrival from the Kisters and Kuder data with the corresponding LOAD\_BLAST\_ENHANCED and CAB results. The Figure 7 comparison indicates that the times-of-arrival provided by LOAD\_BLAST\_ENHANCED significantly delayed compared to the data for points below the triple point, i.e. Mach Stem arrival, but agree fairly well above the triple point. The arrival of the incident wave above the triple point is governed by the portion of the LOAD\_BLAST\_ENHANCED algorithm that is essentially identical to the ConWep function. However, the arrival of the Mach Stem is based on interpolating the UFC 3-340-02 charts, and this is the only known validation of the Mach Stem feature.

The CAB results in the Mach Stem region, below 300mm, indicate a nonlinear vertical speed for the triple point – quite different from the essentially linear speed provided by the Kisters and Kuder data. Above the triple point, the CAB data is in good agreement with both the Kisters and Kuder data and the LOAD\_BLAST\_ENHANCED results, with the exception of the two highest gauge locations. The reasons for these CAB variations from the data are not known.

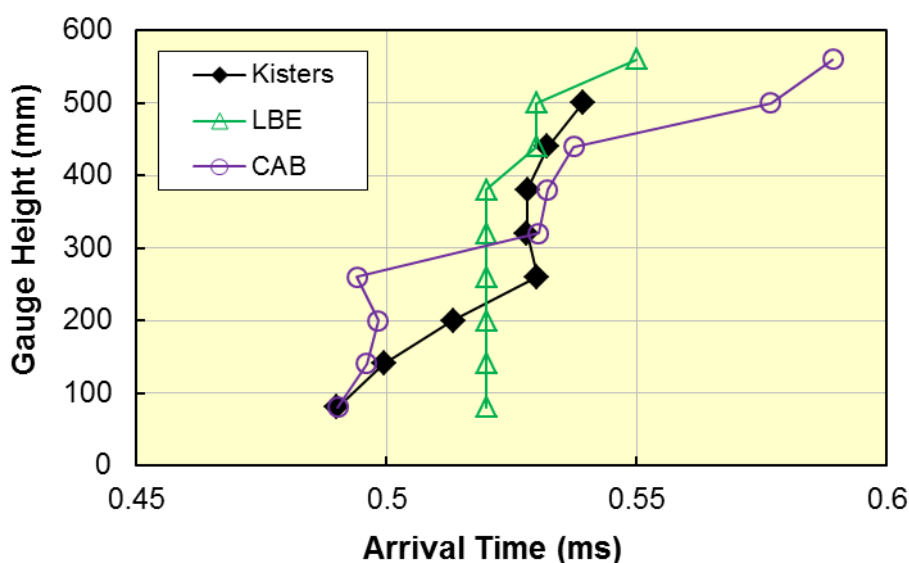


Figure 7 Comparison of time-of-arrival measured by Kisters and Kuder and provided by LOAD\_BLAST\_ENHANCED and CAB engineering models.

#### 4.2 Reflected Wave Arrival Time

The arrival times of the measured, LOAD\_BLAST\_ENHANCED and CAB reflected surface waves are compared in Figure 8. All three curves in Figure 8 have about the same slope (wave speed) of 1400 m/s, but the LOAD\_BLAST\_ENHANCED results are advanced by about 0.5ms.

<sup>4</sup> This figure, and most of the following figures, is plotted in a non-conventional manner with the independent variable (gauge height) on the ordinate rather than the abscissa. The intent is to provide a more easily understood representation of the results.

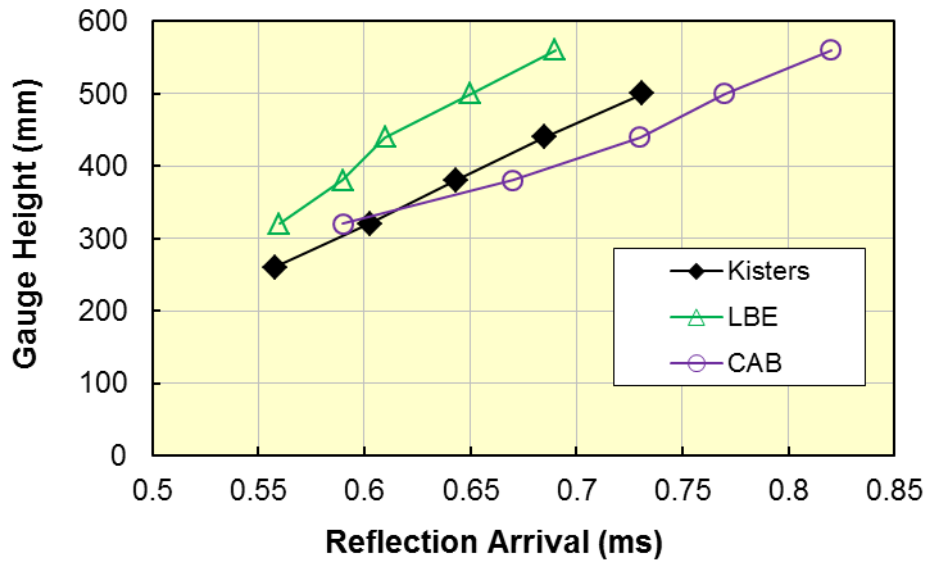


Figure 8 Comparison of reflected wave arrival times measured by Kisters and Kuder and provided by LOAD\_BLAST\_ENHANCED.

Since the LOAD\_BLAST\_ENHANCED reflected wave arrival time is a function of interpolating the UFC 3-340-02 charts, it is likely some reassessment of this interpolation is necessary.

#### 4.3 Maximum Pressures

Kisters and Kuder (2012) acknowledge some difficulty in assessing the maximum pressure in their wave forms:

“Due to sensor ringing this peak pressure could not be simply determined from the measured data.”

None the less, they estimate these pressures and provide a chart of peak pressure versus gauge height; their Figure 7. In general, selecting peak pressures in numerical simulations of shock waves is also problematic, as the sampling rate, especially too coarse (infrequent) a rate, will almost always miss the maximum pressure. Figure 9 compares the Kisters and Kuder measured *first*<sup>5</sup> peak pressures with those provided by the LOAD\_BLAST\_ENHANCED and CAB simulations.

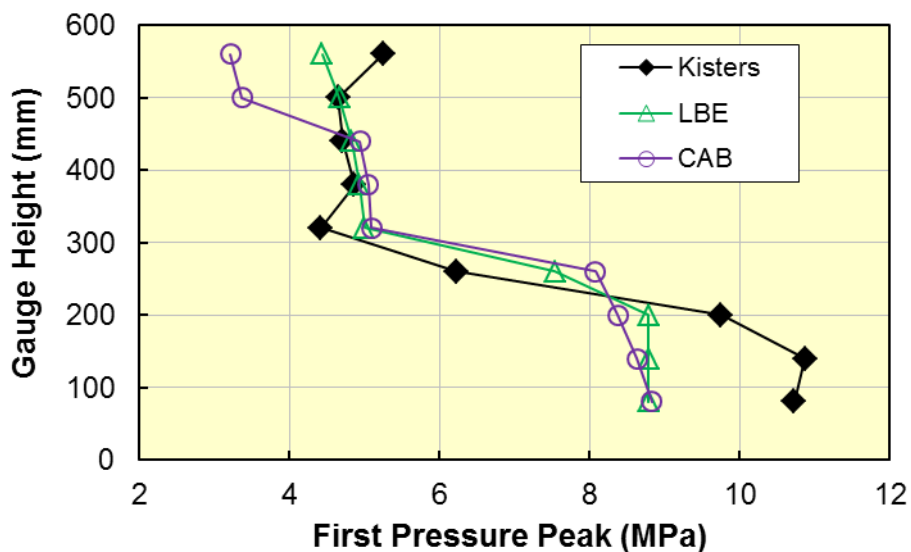


Figure 9 Comparison of first peak pressures measured by Kisters and Kuder and provided by LOAD\_BLAST\_ENHANCED.

<sup>5</sup> The *maximum* pressure is sometimes the reflected pressure arriving after the incident wave.

In this *first* peak pressure comparison, both the `LOAD_BLAST_ENHANCED` and `CAB` results under predict the measured peak pressures in the Mach Stem region, i.e. below 260mm, but provide reasonable agreement with the data above the triple point. Again, the response above the triple point is essentially identical with that from `ConWep` and the response below the triple point is from interpolation of the curves in `UFC-3-340-02`, which has not been otherwise validated.

#### 4.4 Maximum Impulse

A better metric for comparing shock wave results is the impulse, i.e. time integration of the pressure history. Kisters and Kuder provide a chart of measured maximum impulses in their Figure 7. The present Figure 10 compares the Kisters and Kuder measured maximum impulses with those provided by the `LOAD_BLAST_ENHANCED` and `CAB` simulations. The impulses provided by `LOAD_BLAST_ENHANCED` and `CAB`, over predict the Kisters and Kuder measurements in the Mach Stem region (below about 260mm), and significantly over predict the measured impulses above the triple point. This is a reversal in agreement from the arrival times and pressures where agreement below the triple point was suspect.

Referring back to the pressure histories shown previously in Figure 5, the `LOAD_BLAST_ENHANCED` and `CAB` wave forms are quite similar to the Kisters and Kuder data below the triple point at 200mm; although the wave forms are slightly shifted in time with respect to the data. However, above the triple at 320mm, apparently the long duration positive pressure ‘tails’ of the engineering model wave forms contributes significantly to the maximum impulse, which was sampled at 1.5ms to be consistent with the Kisters and Kuder data. The reason for these wave form difference is explored in the subsequent 3D MM-ALE simulation section.

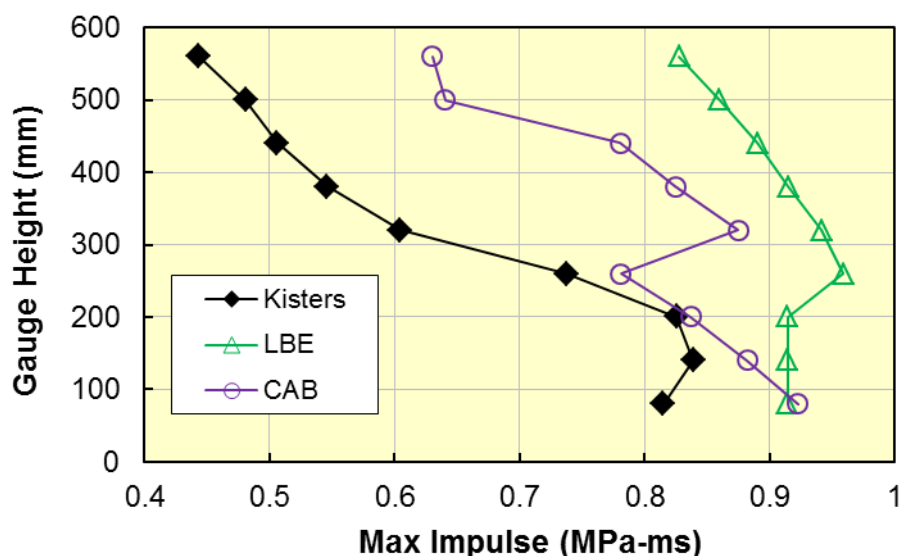


Figure 10 Comparison of maximum impulse measured by Kisters and Kuder and provided by `LOAD_BLAST_ENHANCED` and `CAB` engineering models.

## 5 Multi-Material Arbitrary Lagrangian-Eulerian Modeling and Results

The Kisters and Kuder (2012) experiment was modeled using an axisymmetric geometry and the LS-DYNA Multi-Material Arbitrary Lagrangian-Eulerian (MM-ALE) solver. The axisymmetric geometry included the surface below the charge via a zero vertical velocity boundary condition. The vertical gauge array was modeled as a zero radial velocity boundary condition, spanning from the reflecting surface to a height of 650mm, i.e. the approximate total height of the gauge array shown previously at the right of Figure 1. A consequence of the axisymmetric geometry, and this radial boundary condition, is rather than representing the array as a narrow, approximately 200mm wide, steel strip, the array becomes a circular ring surrounding the charge. While this modeling approximation is likely acceptable

for the initial wave arrival and pressures, it does neglect any clearing effect around the narrow gauge array support, and affects the pressure wave form and evaluation of the impulse. In a subsequent section, the early time axisymmetric results are mapped onto a truncated three dimensional mesh to assess the engineering approximation of using an axisymmetric model.

## 5.1 Model Geometry

The background mesh consists of a square air domain of dimensions 1m in height and 1m in radius. The 1kg TNT charge is located on the axis of symmetry 320mm above the lower surface of the mesh. Figure 11 provides an illustration of the MM-ALE model configuration. The pressures gauge locations are indicated by Tracer Particles along the right boundary. Properties for the air and TNT are provided in an appendix.

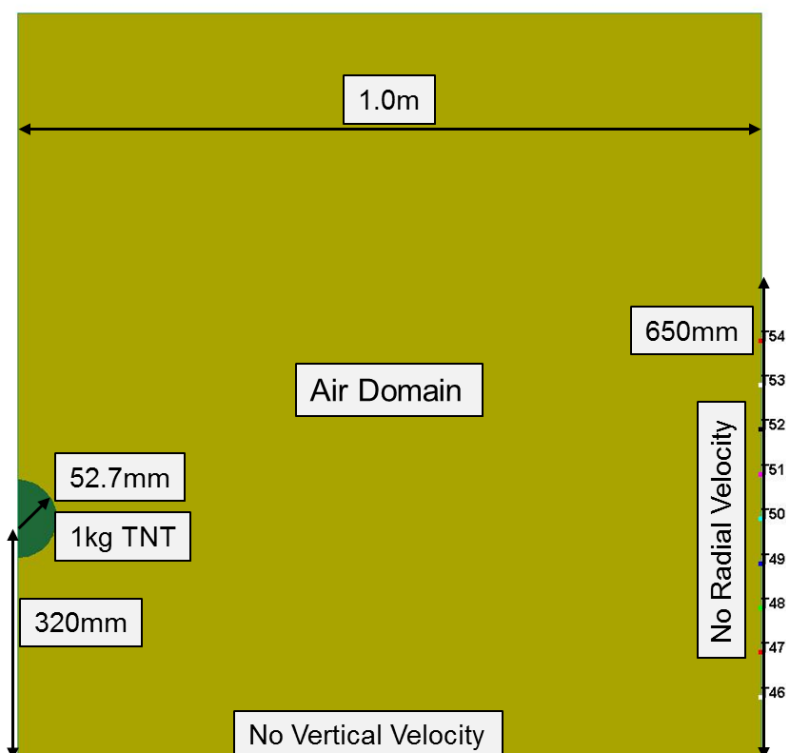


Figure 11 Illustration of the MM-ALE height of burst model configuration.

## 5.2 Mesh Refinement

As with any numerical simulation, an assessment of the discretization error is required. In this case, three mesh configurations were considered, the models consisted of uniformly meshed domains with 4, 2 and 1mm square elements; the resulting number of elements was 62,250, 250,000 and 1,000,000.

As an indication of the mesh convergence, Figure 12 shows the first peak pressures at the nine gauge heights for the three mesh discretizations. While the MM-ALE results appear to be converging in the region above the triple point, i.e. 300mm and greater, they are converging more slowly below the triple point. The Kisters and Kuder (2012) results are included as a reference. Below the triple point, in the Mach Stem region, the convergence toward the measured results indicates significant change with mesh refinement, and apparently requires additional mesh refinement beyond the 1mm mesh simulation. The reason for the very poor pressure results at the lowest gauge location, i.e. 80mm, for all three MM-ALE mesh refinements is not known.

As noted earlier, there is some uncertainty in assessing the peak pressure in both the measurements and simulations, while convergence of the MM-ALE results to the Kisters and Kuder measurements is not a requirement, it would certainly be desirable.

The 4mm mesh required only 16 minutes of CPU for the simulation duration of 1.5ms, slightly more than 2 hours for the 2mm mesh, and 13.5 hours for the 1mm mesh, all on the same single processor Windows based PC<sup>6</sup> LS-DYNA development version 77817 double precision.

The MM-ALE results presented in subsequent sections are for the 1mm mesh.

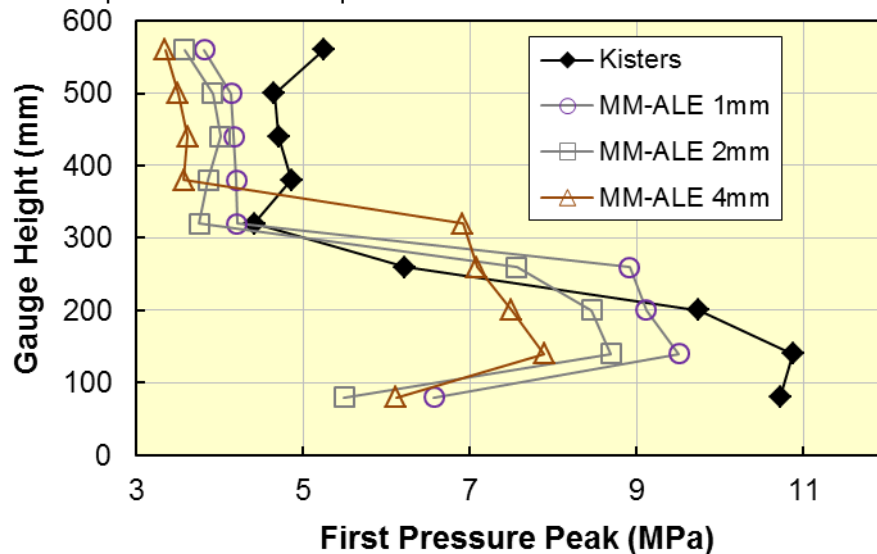


Figure 12 Comparison of first peak pressures measured by Kisters and Kuder with three MM-ALE mesh refinements.

### 5.3 Time-of-Arrival

Figure 13 compares the times-of-arrival for the first arriving wave measured by Kisters and Kuder, and from the LOAD\_BLAST\_ENHANCED, CAB and MM-ALE models; all but the latter results were previously compared in Figure 7. The MM-ALE result indicates slightly later arrival times in the Mach Stem region, i.e. at and below 260mm, than the measured arrival times. The later arrival times for the MM-ALE result persist above the triple point and the delay increases with the height of the measurement. The 2 and 4mm mesh refinement MM-ALE models provided similar times-of-arrival as the 1mm model results.

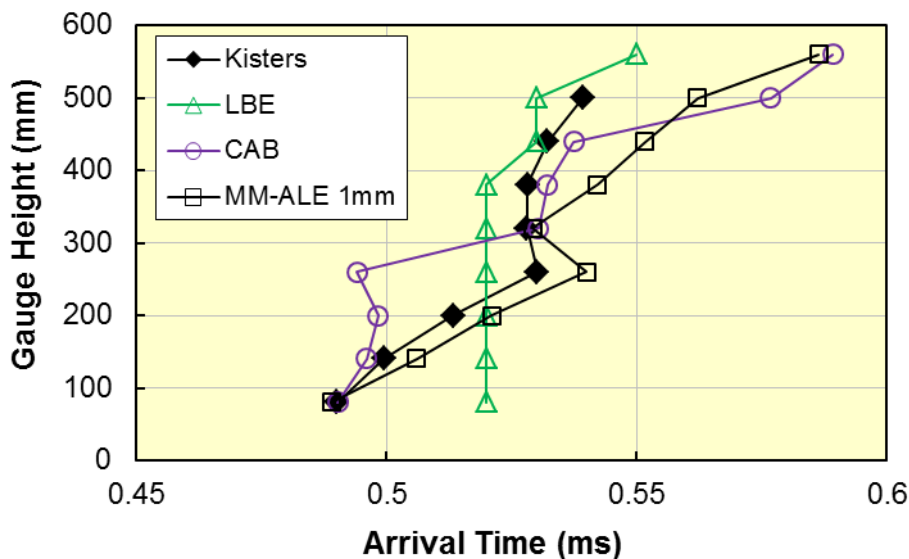


Figure 13 Comparison of times-of-arrival measured by Kisters and Kuder and provided by LOAD\_BLAST\_ENHANCED, CAB and 1mm MM-ALE models.

<sup>6</sup> The LOAD\_BLAST\_ENHANCED results required only 2 seconds of CPU time.

#### 5.4 Reflected Wave Arrival Time

Figure 14 compares the reflected wave arrival times measured by Kisters and Kuder, with those from the LOAD\_BLAST\_ENHANCED, CAB and MM-ALE models; all but the latter result were previously compared in Figure 8. The reflected wave in the MM-ALE simulation travels up the vertical gauge array somewhat slower, about 880m/s, than the 1400m/s for both the measurements and LOAD\_BLAST\_ENHANCED results, and 1000m/s CAB result. Also, the MM-

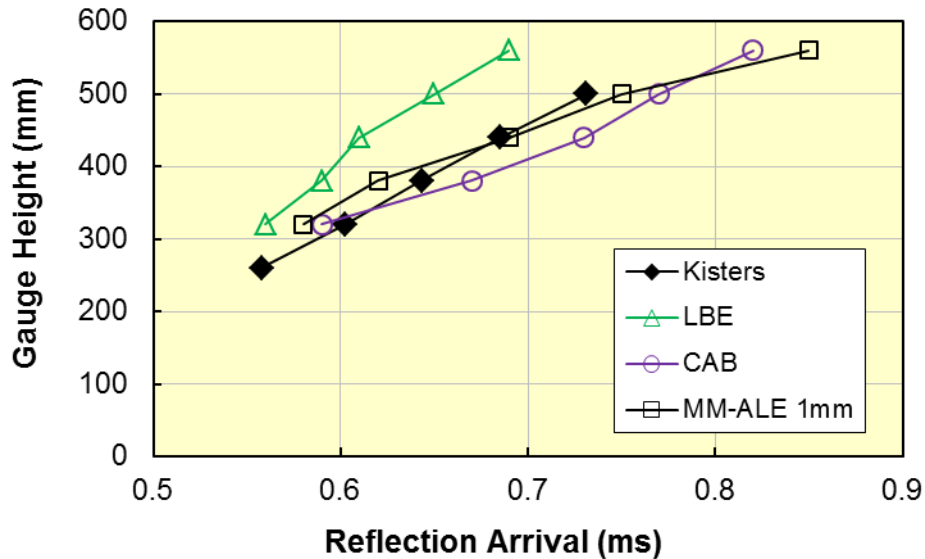


Figure 14 Comparison of reflected wave arrival times measured by Kisters and Kuder and provided by LOAD\_BLAST\_ENHANCED, CAB and 1mm MM-ALE models.

ALE results do not indicate a reflected wave at the 260mm gauge location – implying the triple point is above 260mm, but below 300mm, for this simulation.

#### 5.5 Maximum Pressures

Figure 15 compares the peak pressures, for the first arriving wave, measured by Kisters and Kuder, and from the LOAD\_BLAST\_ENHANCED, CAB and MM-ALE models; all but the latter results were previously compared in Figure 9.

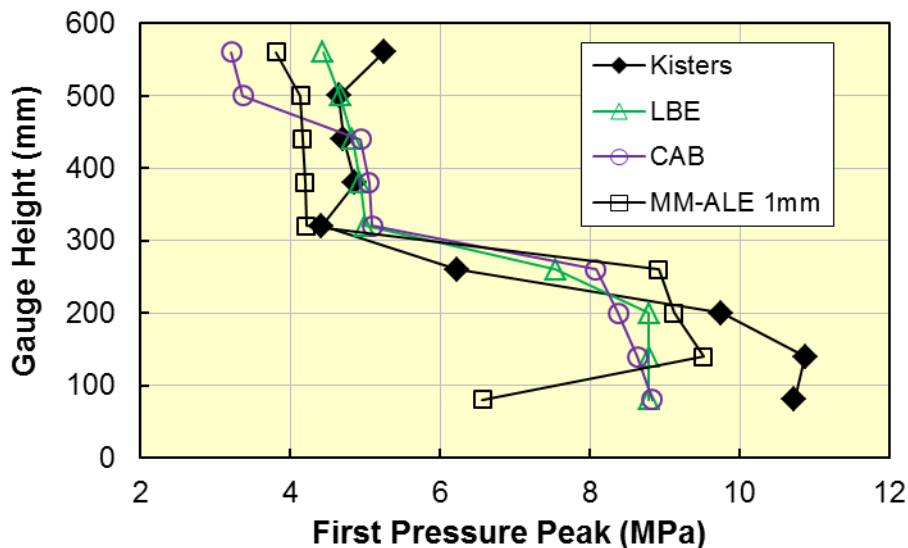


Figure 15 Comparison of peak pressure of the first arriving wave by Kisters and Kuder and provided by LOAD\_BLAST\_ENHANCED, CAB and 1mm MM-ALE models.

As mentioned, the determination of the peak pressure is difficult. However, the estimated first wave peak values, as shown in Figure 14, do provide a good indication of where the triple point occurs. All the model results and the data indicate the triple point is below the gauge at 320mm.

Figure 16, shows the pressure histories for the 260mm gauge location from the Kisters and Kuder data and the MM-ALE result for the 1mm mesh. The data clearly indicates the arrival of the reflected wave shortly after the first (incident) wave arrival. Thus the triple point is below the 260mm gauge location based on this measurement. The MM-ALE pressure history does not indicate a second (reflected) wave and hence the triple point is above the 260mm location.

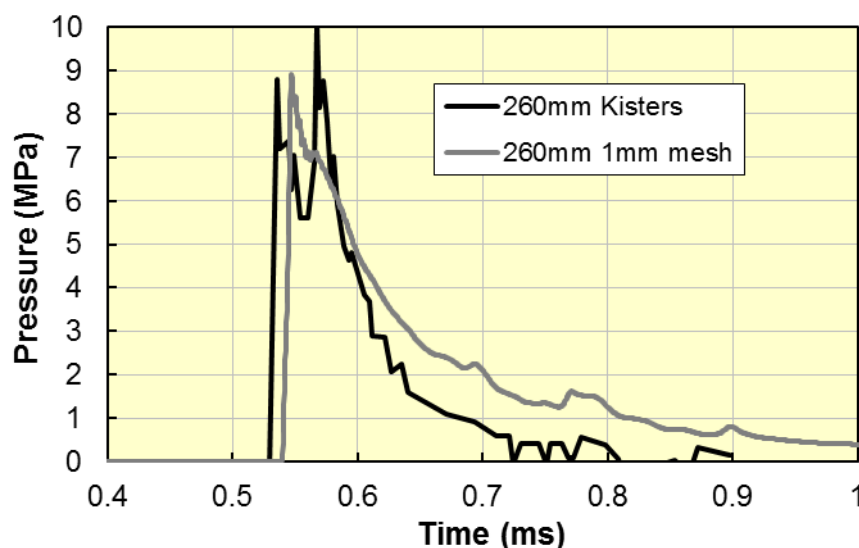


Figure 16 Comparison of pressure histories for the gauge 260mm above the reflecting surface for the Kisters and Kuder measurement and the 1mm mesh MM-ALE model.

## 5.6 Maximum Impulse

Figure 17 compares the maximum impulse measured by Kisters and Kuder, and the LOAD\_BLAST\_ENHANCED, CAB and MM-ALE<sup>7</sup> models; all but the latter results were previously compared in Figure 10. On average, the MM-ALE impulses overestimate the measured impulses by about 39%, with a coefficient of variation of about 40%. For most structural analysis simulations impulse is the most important blast wave characteristic, when assessing structural vulnerability or lethality. An impulse over prediction of 39% should not be ignored in an application of the MM-ALE solver to Mach Stem loading scenarios. It is likely the combination of the axisymmetric geometry and especially the *constrained radial velocity* along the gauge array prevents appropriate clearing action around the gauge array and the result is increased impulses in the simulation. Note: the MM-ALE impulse results have a shape similar to those measured by Kisters and Kuder, but offset (greater) by about 0.25 MPa-ms.

A 3D model would be required to allow for clearing around the narrow gauge array. Then an assessment about clearing affecting the model impulses would be possible. The results from a simple 3D model are provided in a subsequent section.

<sup>7</sup> The impulses were sampled at 1.5ms before any reflection from the upper surface arrived at the 560mm gauge height. Kisters and Kuder also sampled their impulse histories at 1.5ms when impulse plateaus were obtained.

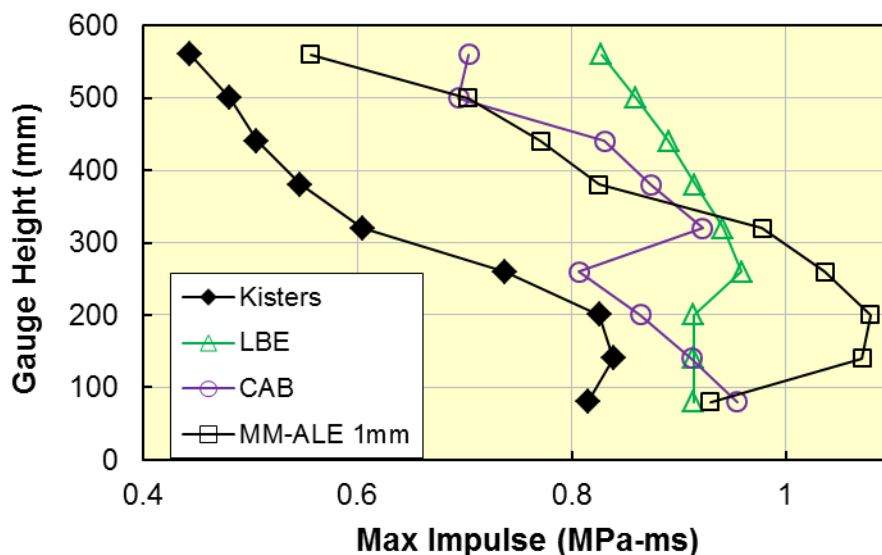


Figure 17 Comparison of maximum impulses measured by Kisters and Kuder and provided by LOAD\_BLAST\_ENHANCED, CAB and 1mm MM-ALE models.

## 6 MM-ALE Mapping

The previous MM-ALE simulations were run with uniformly meshed square elements of side length dimensions 4, 2 and 1mm, comprising the axisymmetric air and spherical explosive charge domains. An alternative solution strategy is to use an initial 1D spherically symmetric mesh to model the air and explosive charge domain, but only to a radius equal to the height of burst, i.e. 320mm. This simulation is terminated just before the shock wave arrives at the end of this mesh, i.e. just before the shock wave interacts with the rigid reflecting surface. This 1D spherically symmetric solution is then be mapped onto an axisymmetric 2D mesh and the simulation continued.

This process is referred to as MM-ALE mapping or simply mapping; see Aquelet and Souli, (2008). The results from the initial run, e.g. 1D spherically symmetric, are saved to a map file by including the "map=" on the LS-DYNA execution line, e.g. LS-DYNA.exe i=My1DInput.k map=1Dmap. In the subsequent run, when the mapped file is to be read the execution line is similar LS-DYNA.exe i=My2DInput.k map=1Dmap and the new input file (My2DInput.k) contains the keyword \*INITIAL\_ALE\_MAPPING which provides the instructions for mapping the 1D spherical result onto the 2D mesh, e.g. what ALE-MULTI-MATERIAL\_GROUPS from the 1D simulation are mapped to the 2D ALE-MULTI-MATERIAL\_GROUPS and the location of the origin of the 1D result in the 2D mesh. Note: the original Aquelet and Souli 2D to 3D mapping function has been expanded to include 1D mapping to 2D and 3D geometries, and other combinations.

The primary reason for considering mapping in MM-ALE simulations is the ability to use highly refined meshes in the lower dimensional geometry, i.e. a fine mesh 1D result is mapped onto a more coarse 2D mesh. This approach obviously saves CPU time, but there is an expected loss in accuracy due to the mapping operation, and the use of a more coarse mesh in the mapped solution. The analyst needs to decide how many mapping operations are needed, and most importantly, the refinement level of the mesh onto which the previous result is mapped.

There is little guidance in the literature on selecting relative mesh refinement ratios. In part because this choice is problem dependent, e.g. optimal mapping ratios for shocks in water will differ from those needed for air shocks. Additionally, the allowable or tolerable amount of error due to mapping is application dependent.

The paper by Lapoujade et al. (2010) provides some comparisons of 2D to 3D mappings for a free air burst. The comparisons include pressure wave forms and impulses for different ratios of 3D/2D mesh

densities spanning a ratio range of 1 to 25. They conclude, if maximum pressure is important a ratio less than 15 is recommended, and if impulse is important a ratio of 20 or less is recommended.

In this section, results of a similar mapping mesh ratio study are presented. The focus is on the impulse at the same nine vertical gauge locations examined in the previous sections. In the first subsection, the results from a 1D spherically symmetric model using, 1mm mesh spacing, are mapped onto the 4, 2 and 1mm 2D axisymmetric meshes used previously. In the second section, the results of the three 2D axisymmetric meshes are mapped onto a simplified 3D mesh of 5mm elements. These 3D mesh results provide some insight into the clearing effects that were ignored in the previous 2D axisymmetric results for the impulses.

## 6.1 1D to 2D MM-ALE Mapping

A 1D spherically symmetric model was used to generate the initial detonation of the TNT and expansion of the air and detonation products. The model consisted of 320 beam elements of length 1mm and was run for a duration of 0.076ms, i.e. just before the shock wave reached the end of the mesh where the rigid reflecting surface will be modeled in the 2D axisymmetric simulation. The inputs for this MM-ALE model are essentially identical to those used in other MM-ALE models to include the ability to fill the explosive region using the INITIAL\_VOLUME\_FRACTION\_GEOMETRY keyword and inclusion of tracer particles. The 1D spherical geometry is indicated via the SECTION\_ALE1D keyword and the parameter ELFORM=-8, where the negative eight indicates spherical symmetry; other 1D geometries are available. Included on the LS-DYNA execution line is the indication a mapped results file is requested via the entry "map=1D-1mm" the file name is arbitrary but the use of some mnemonics in the file name is helpful, especially if multiple mappings are considered.

As mentioned above, the mapped results file from the 1D spherical simulation are then mapped onto the three 2D axisymmetric meshes, e.g. mesh sizes 4, 2 and 1 mm. Since both the 1D spherical and 2D axisymmetric models only have two ALE-MULTI-MATERIAL\_GROUPS, i.e. the TNT and air, the required mapping keywords are straightforward.

In the present case, the 2D axisymmetric background mesh is defined to be air, via a PART keyword. However, the INITIAL\_VOLUME\_FRACTION\_GEOMETRY keyword can be used to initially fill the background mesh before the application of the mapped results over writes those parts of the background mesh it covers. As an example, if sand was to replace the present model's rigid surface, INITIAL\_VOLUME\_FRACTION\_GEOMETRY keyword could be used to define the background mesh as air with soil near the bottom. The mapped file results would then initialize the applicable portion of the mesh, e.g. the 320mm radius from the center of the TNT charge.

The LS-DYNA keyword that indicates mapping from a previous simulation is to be applied is INITIAL\_ALE\_MAPPING which opens the mapped results file indicated on the execution line "map=1D-1mm," i.e. the 1D spherical results. Note: *without* the INITIAL\_ALE\_MAPPING keyword in the 2D input file, this "map=" file name would be written at the end of the 2D simulation.

When the mapped results file is read by LS-DYNA, there will be two or more ALE-MULTI-MATERIAL\_GROUPS and instructions must be provided as to how these 1D ALE-MULTI-MATERIAL\_GROUPS relate to the ALE-MULTI-MATERIAL\_GROUPS in the 2D input. This is accomplished via the parameters that define the INITIAL\_ALE\_MAPPING keyword:

```
*INITIAL_ALE_MAPPING
$  PID  TYP  AMMSID
   100,  1, 10010
$  XO   YO   ZO  VECID ANGLE
   0.0, &HOB, 0.0, 222
```

where the PID and TYP parameters define the background mesh, and AMMSID points to a SET\_MULTI-MATERIAL\_GROUP\_LIST that defines the 2D ALE-MULTI-

MATERIAL\_GROUPS corresponding to those in the 1D mapped results file. It is important to recall the ALE-MULTI-MATERIAL\_GROUPS are not referenced by PART ID, but rather their order of appearance, ordinal number<sup>8</sup>. The following SET\_MULTI-MATERIAL\_GROUP\_LIST keyword

```
*SET_MULTI-MATERIAL_GROUP_LIST
$ AMSID
  10010
$ AMGID1 AMGID2
  1,    2
```

tells LS-DYNA the first ALE-MULTI-MATERIAL\_GROUP from the 1D mapped results file should be mapped onto the first ALE-MULTI-MATERIAL\_GROUP of the 2D simulation and similarly for the second groups. For the present example this is trivial, but again consider the case where there is air and a soil layer rather than a rigid surface. In the 2D input the air is the first ALE-MULTI-MATERIAL\_GROUP and the soil is the second, then the SET\_MULTI-MATERIAL\_GROUP\_LIST keyword would be

```
*SET_MULTI-MATERIAL_GROUP_LIST
$ AMSID
  10010
$ AMGID1 AMGID2
  1,    1
```

That is both the explosive and air from the 1D spherical simulation should be mapped to the air ALE-MULTI-MATERIAL\_GROUP in the 2D simulation; where it is assumed the air is the first ALE-MULTI-MATERIAL\_GROUP defined in the 2D simulation.

Finally, the mapped results must be positioned within the 2D model. This is accomplished via the second line of parameters defining the INITIAL\_ALE\_MAPPING keyword. The parameters XO, YO, ZO provide the coordinates in the 2D model where the origin from the 1D simulation is to be located. The orientation of the mapped results is provided by defining a vector whose ID is given as the parameter VECID. While the keyword DEFINE\_VECTOR is always required in any mapping operation, it is ignored in 1D-to-2D and 2D-to-2D mappings as the X-Y plane is assumed with the Y-axis the axis of asymmetry.

Figure 18 compares pressure fringes at 0.076ms for the 2D 4mm mesh without mapping (left side) with the mapped 1D 1mm mesh solution (right side). In addition to be perfectly symmetric, the mapped pressure fringes also indicate high pressures region (red fringe > 8MPa) is more uniform than the no mapping fringes. The extent of the outer most pressure fringe also is slightly greater for the mapped case than without mapping; in air blast the larger the pressure the faster the shock wave propagation speed.

---

<sup>8</sup> A number that indicates position or order in relation to other numbers: first, second, third, etc.

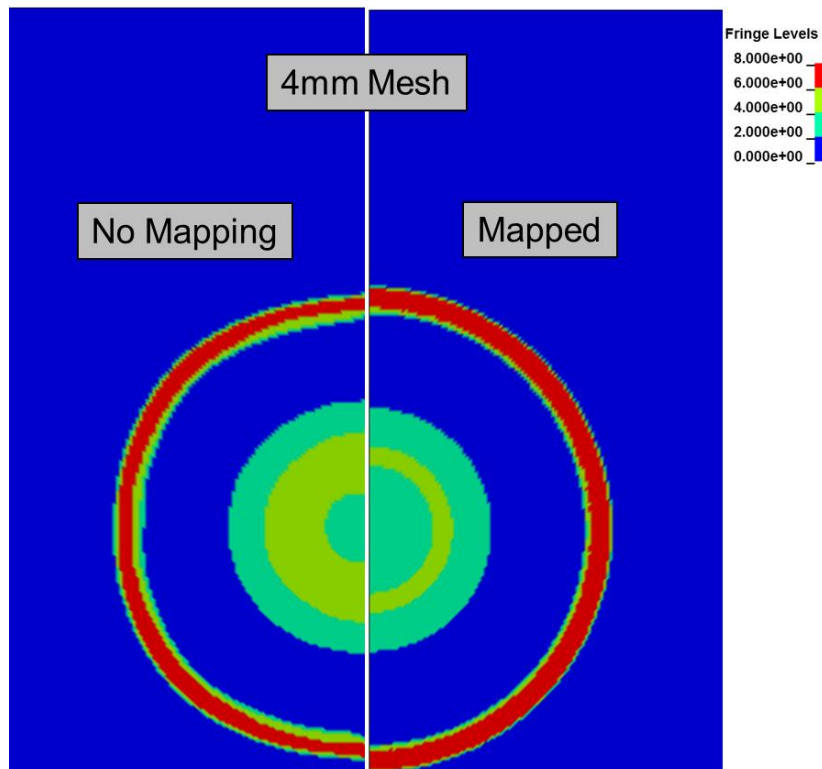


Figure 18 Comparison of pressure fringes from the 2D 4mm mesh without mapping (left) and mapping of the 1D 1mm mesh (right) results at 0.076ms.

Mapping the 1D 1mm solution onto the three 2D mesh refinements does not produce much difference in the maximum impulses at the gauge locations. Figure 18 compares the three 2D mesh refinement maximum impulses with the Kisters and Kuder data. However, some small improvement in agreement with the data is obtained when the mapped results are compared with the no-mapping results, as shown in Figure 19. The maximum impulses from the mapped solution are slightly less at all the gauge locations other than the highest gauge at 560mm.

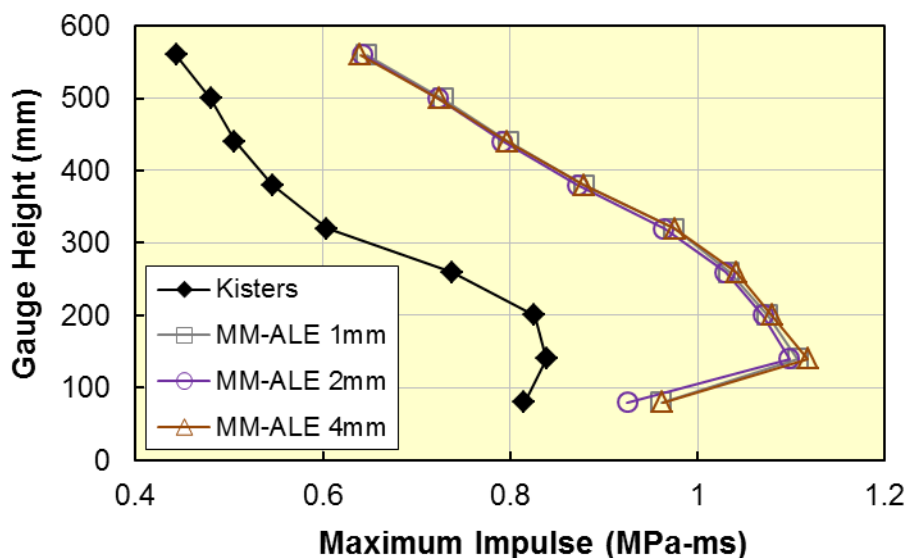


Figure 19 Comparison of maximum impulse for the Kisters and Kuder data and the three mesh refinements using the mapped 1D 1mm results.

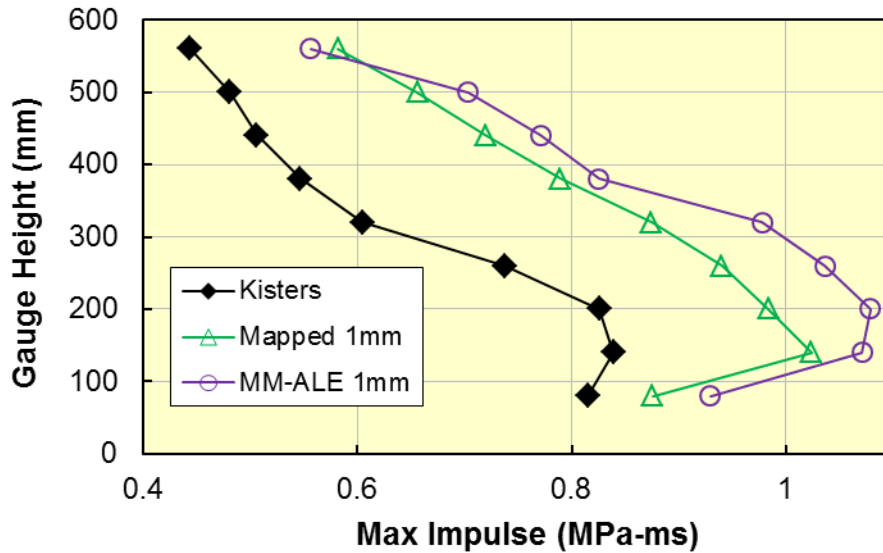


Figure 20 Comparison of maximum impulse for the Kisters and Kuder data and the 2D 1mm mesh refinements results with and without mapping of the 1D 1mm results.

The bar chart shown in Figure 21 compares the maximum impulse average relative error, with respect to the Kisters and Kuder data, for the maximum impulses from the mapped, using the 1D 1mm results, and no mapping models for the three mesh refinements considered. This chart clearly indicates the mapped solutions provide average results closer to the measured data.

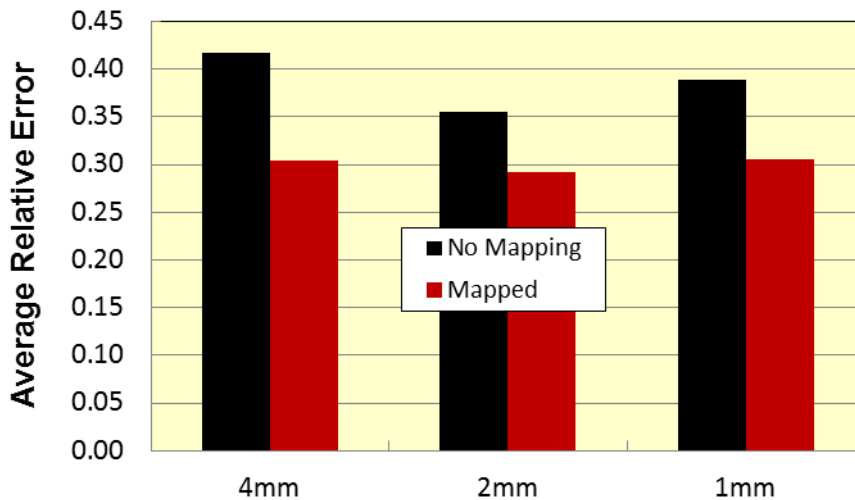


Figure 21 Comparison of maximum impulse average relative error for three mesh refinements with and without mapping.

However, while minimizing the relative error is important, the other practical consideration is the CPU required to obtain a solution. Figure 22 compares the CPU time, in minutes, for the three mesh refinements with and without mapping; the 1D 1mm solution took only about 1 minute. The 2mm mesh took more than seven times as much CPU time as the 4mm mesh, and the 1mm mesh required about 57 times as much CPU as the 4mm mesh. Balancing this CPU time comparison with the above maximum impulse relative error, it is obvious that the mapped solution onto the 4mm mesh is optimal for these parameters.

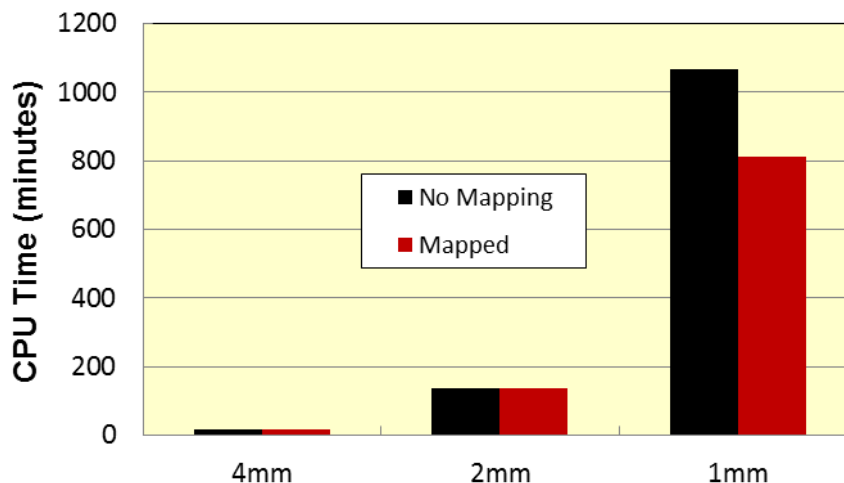


Figure 22 Comparison of CPU time for three mesh refinements with and without mapping.

## 6.2 1D to 2D to 3D MM-ALE Mapping

As mentioned previously, the 2D axisymmetric model does not allow for clearing of the pressure around the vertical gauge array, as the no radial velocity boundary condition acts to contain the pressure in the vicinity of the gauge array. Containment of the pressure contributes to an increase in the impulse in the 2D MM-ALE simulations. To assess the effect of the pressure confinement, the 2D axisymmetric results are mapped onto a reduced 3D mesh.

Figure 23 shows the reduced 3D model consisting of a rectangular air domain of dimensions 1500x1500x500mm. The half-symmetry gauge array is located 1000mm from the origin with 500mm of air domain behind the array, 400mm of air domain to the side, and 850mm of air domain above. Recall the gauge array width was 200mm and the height was 650mm. The gauge array is implemented in the MM-ALE simulation by locating the array on mesh lines within the air domain and constraining all velocity components on the plane representing the gauge array.

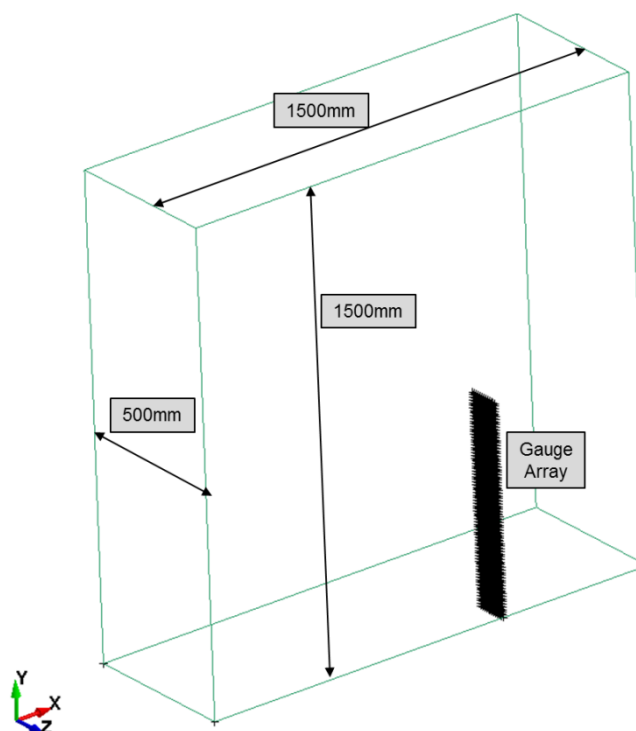


Figure 23 Illustration of reduced 3D model.

The other boundary conditions are no X-velocity on the YZ-plane on left end of the domain, No Y-velocity on the XZ-plane at the bottom of the domain, and no Z-velocity on the two planes parallel to the XY-plane. The top and right side of the domain have prescribed one atmosphere pressure boundary conditions.

Three uniform 3D mesh refinements were considered: 20, 10 and 8mm. The uniform 8mm mesh with more than 21 million elements was basically just below the memory limit for the Windows based PC used in this study. Only the results from the uniform 8mm mesh are presented in this subsection. Alternate meshing approaches were not considered, as the goal of the 3D simulations was to assess the pressure clearing affect on the impulses.

The three 2D axisymmetric meshes were initialized with the 1D 1mm results, as discussed above, and then run for a short duration of 0.45 ms which is just before the shock waves interact with the gauge array. The 2D mesh results were then mapped onto the 3D 8mm mesh and the simulations continued to the 1.5ms termination time. The mapping sequence is similar to that for the 1D to 2D and is provided in an appendix.

Figure 24 shows fringes of pressure in the 3D 1mm mesh. The left most image is the initial mapping of the 2D 1mm mesh results at 0.45ms, just before the pressure wave reaches the gauge array. Note the upper portion of the circular pressure wave is truncated because the 2D mesh was only 1000mm in height and the 3D mesh is 1500mm in height.

The right image, in Figure 24, shows fringes of pressure at 0.82ms when the pressure wave has interacted with the gauge array (straight black line). This image shows the pressure fringe extending beyond the gauge array, as in this 3D model the width of the gauge array is finite.

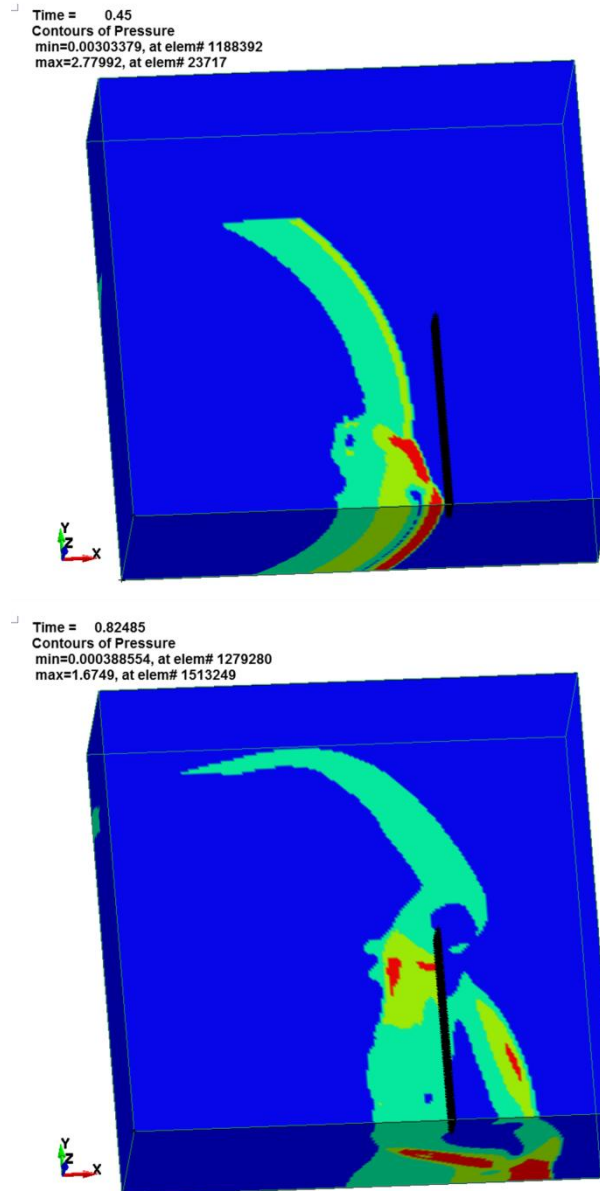


Figure 24 Pressure fringes in 3D mesh for initial mapping at 0.45ms (left) and after interaction with gauge array at 0.82ms (right).

Mapping the three mesh refinement 2D axisymmetric results onto the 3D 8mm mesh produces essentially the same maximum impulse distribution, as shown in Figure 25. However, the 3D maximum impulse distribution is much closer to the Kisters and Kuder data, as shown in Figure 26, than the previous reported 2D axisymmetric maximum impulse distribution.

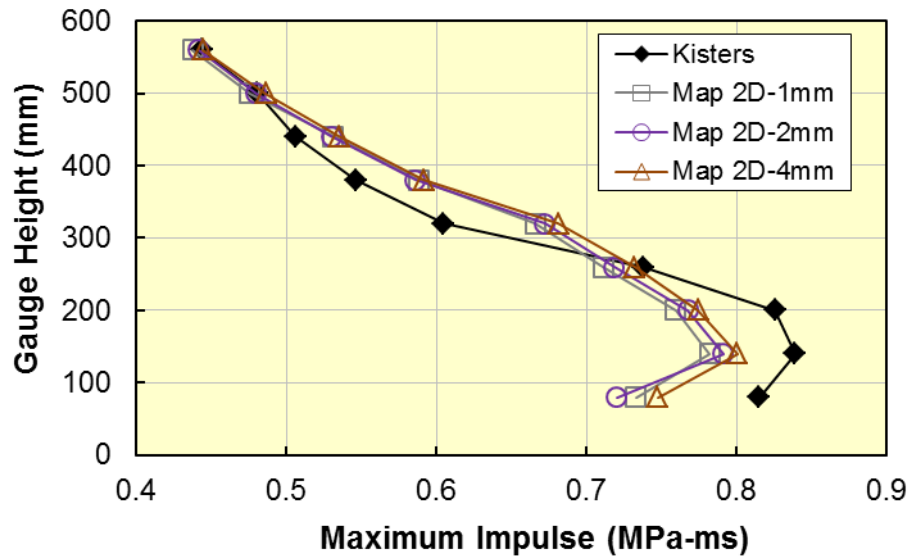


Figure 25 Comparison of maximum impulses for the 3D 8mm mesh using three mesh refinement 2D mapping results.

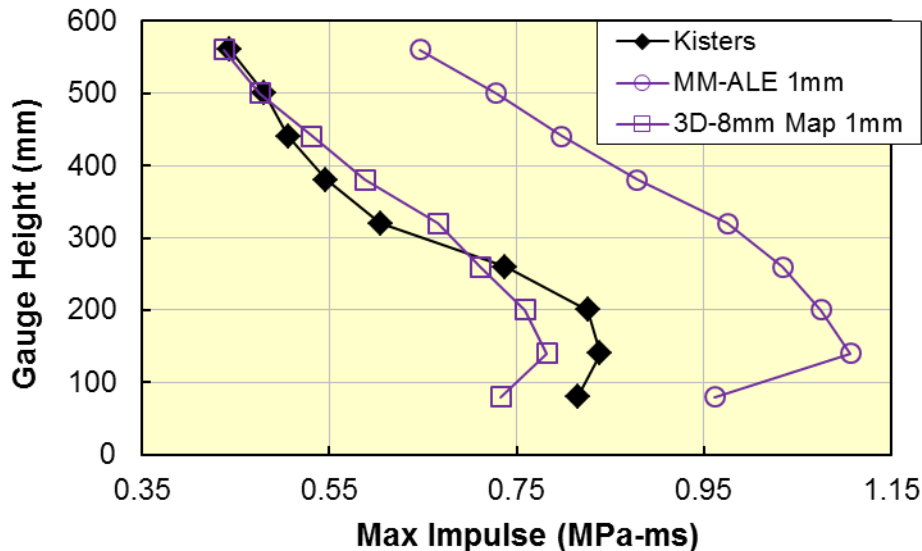


Figure 26 Comparison of maximum impulse distributions from the 2D axisymmetric and 3D mapped MM-ALE models with the Kisters and Kuder data.

The 3D maximum impulse comparison shown in Figure 26 supports the suggestion that the 2D axisymmetric models ignore clearing effects, and hence results in increased maximum impulses. However, the 8mm mesh used in the 3D simulation is quite coarse and results in the loss of the pressure peak and rapid rise to the peak pressure associated with shock waves. The 'tail' of the 3D pressure history, shown in Figure 27, decays more rapidly, in a manner similar to the Kisters and Kuder data, than the 2D axisymmetric pressure history. The more rapid pressure decay for the 3D model is attributed to the clearing effect, and not the more coarse mesh.

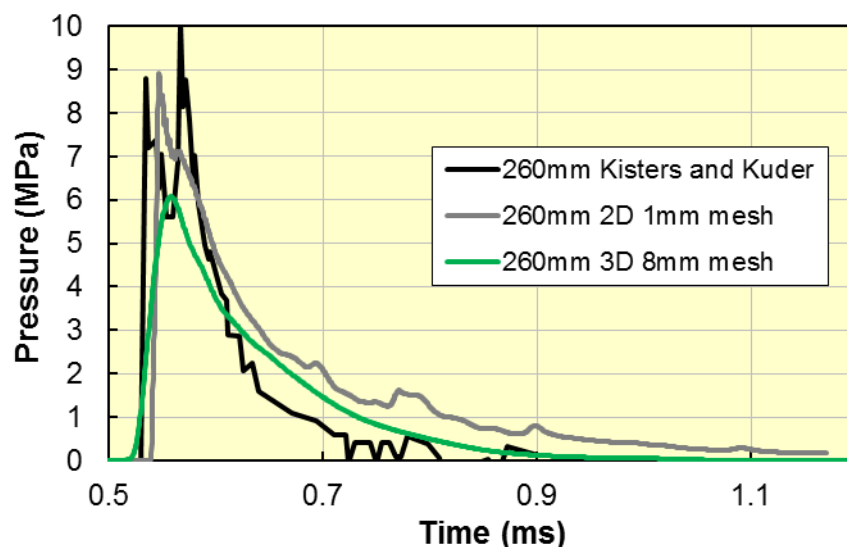


Figure 27 Comparison of pressure histories at 260mm from the 2D and 3D MM-ALE models and the Kisters and Kuder data.

## 7 Horizontal Surface Maximum Pressures

The pressure measurements made by Kisters & Kuder were for gauges in and above the Mach Stem, at a range of 1 meter from the explosive charge. No measurements were made on the horizontal surface below the explosive charge. While most height of bursts experiments, and simulations, are focused on above ground structures, there are scenarios where shallow buried structures may be subjected to surface or height of burst explosions. The LOAD\_BLAST\_ENHANCED and Multi-Material Arbitrary Lagrangian Eulerian simulations detailed above for the Kisters & Kuder experiments, serve to provide *estimates* of the horizontal pressures.

Lacking experimental data for a comparison of horizontal pressures, use will be made of the information provided in UCF 3-340-02 5 (2005), in particular Figure 2-193, reproduced here as Figure 28. This figure provides reflection coefficients versus angle of incidence<sup>9</sup> for various incident pressures. Although UCF 3-340-02 5 does not state if this chart is based on experiments or numerical simulations, it is likely based on the latter.

Mach Stems typically form in the 40 to 50 degree range depending on the height of burst and amount of explosive. Indeed, the data in this figure is used in a height-of-burst example, Example Problem 2A-10, presented in UCF 3-340-02 5.

<sup>9</sup> Angle formed by the normal to the surface that passes through the center of the elevated charge and a line connecting the center of the charge to the surface point of interest.

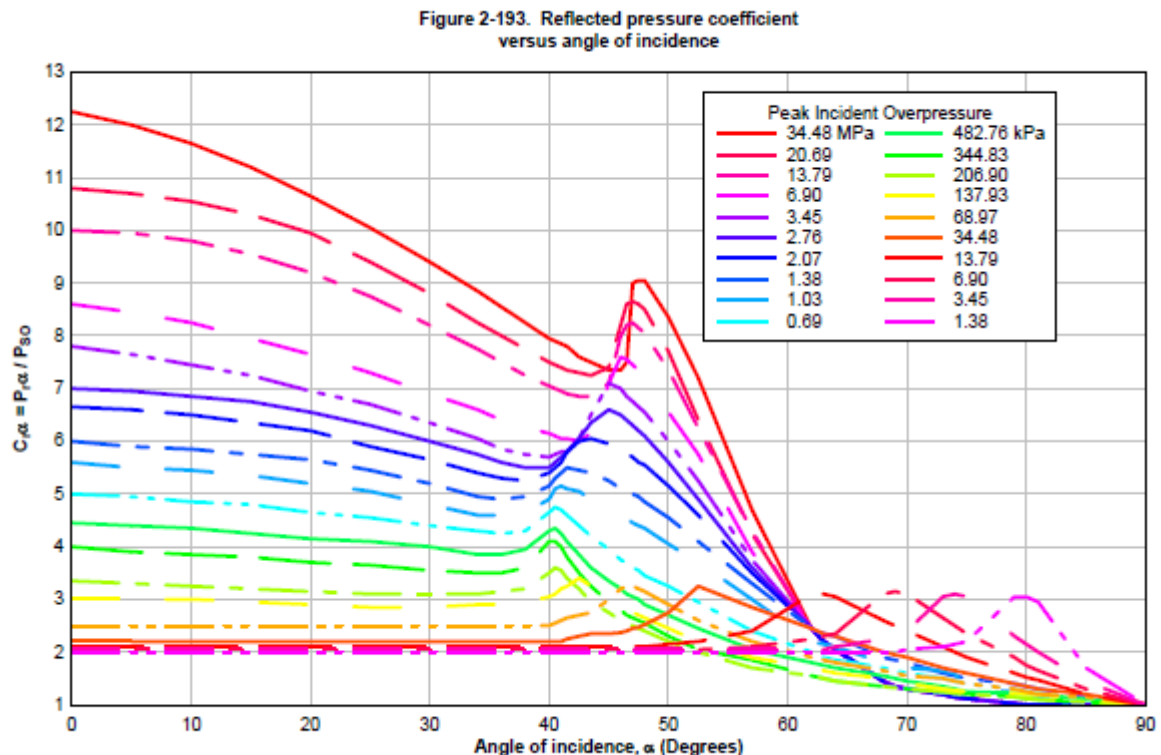


Figure 28 Reflected pressure coefficients versus Angle of Incidence (Figure 2-193 in UFC 3-340-02).

In the `LOAD_BLAST_ENHANCED` and `MM-ALE` height-of-burst simulations, described previously, the pressure histories along the horizontal surface were sampled every 20mm. To obtain the incident pressures needed to use Figure 28, the calculations were repeated. For the `LOAD_BLAST_ENHANCED` case, the type of burst was changed from `BLAST=4` for height-of-burst to `BLAST=2` for a free air burst on the `LOAD_BLAST_ENHANCED` keyword. For the `MM-ALE` case, the axisymmetric mesh was extended an additional 500mm below the original horizontal surface. This domain addition was sufficient to record the maximum pressure at the horizontal plane of interest, without a reflection from the bottom of the extended mesh.

Figure 29 compares the reflection coefficients, i.e. ratio of reflected to incident pressure, from the `LOAD_BLAST_ENHANCED` and `MM-ALE` simulations. The `LOAD_BLAST_ENHANCED` simulation result for zero degrees, i.e. directly under the charge, is questionable since the scaled range to this point is slightly less than recommended in the UCF data; this was mentioned previously in the `LOAD_BLAST_ENHANCED` section. The `MM-ALE` results have a sharp increase at 14 degrees, from a pressure ratio level of about eight, and then trend with the `LOAD_BLAST_ENHANCED` results for larger angles of incidence. It is worth noting again, maximum pressures, in this case both incident and reflected, are difficult to capture due to finite sampling rates of the results.

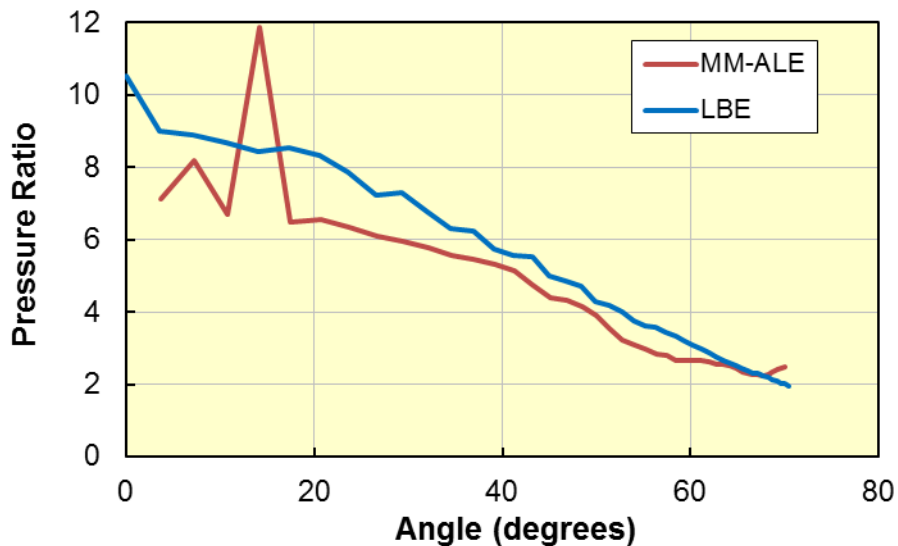


Figure 29 Reflection coefficients versus angle of incidence from the MM-ALE and LOAD\_BLAST\_ENHANCED simulations of a 1 kg TNT charge at 320mm above the surface.

The results shown in Figure 29 are not at a constant incident pressure as are the results from Figure 28, i.e. the UCF 3-340-02 5 results. Using the maximum incident pressures from the MM-ALE simulation, and corresponding angles of incidence, the reflection coefficients in Figure 28 were interpolated, both in incident pressure and angle of incidence, to provide reflection coefficients that can be directly compared with those shown in Figure 29. A comparison of all three reflection coefficients as a function of angle of incidence is shown in Figure 30.

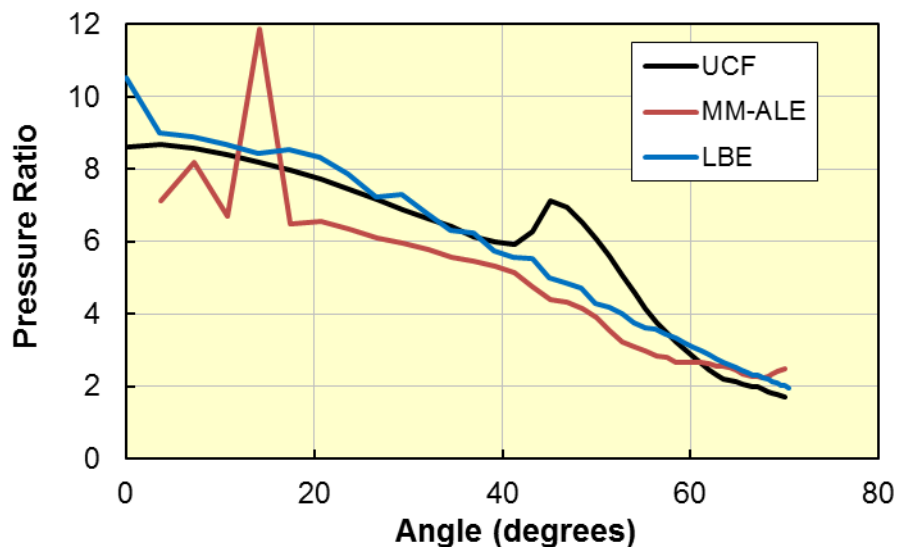


Figure 30 Reflection coefficients versus angle of incidence from UCF 3-340-02 5, MM-ALE and LOAD\_BLAST\_ENHANCED simulations.

The reflection coefficient comparison shown in Figure 30 provides some confidence that the LBE and MM-ALE results are reasonable. The increase in reflection coefficient for the UCF 3-340-02 5 results between 40 and 50 degrees indicates that the Mach Stem is forming at that angle of incidence (range). The MM-ALE results indicate the Mach Stem begins closer to 14 degrees. Again, the start of the Mach Stem depends on both the amount and height of the explosive. The UCF 3-340-02 5 document provides no guidance on what the limits of applicability are for results shown in Figure 28.

## 8 Conclusions

The data presented by Kisters and Kuder is thought to be a good representation of what happens in the reported experiment. There is no reason to doubt their data as they have duplicate vertical array measurements, repeated the experiment three times and have extensive experience as experimentalist, also with similar types of experiments. Their measurements would garner even more confidence had they provided an accuracy assessment of their measurements – they did cite a less than 10% error estimate for the first peak pressures. Further, in their defense, the experiments were not intended as validation experiments, but rather they attempted difficult measurements in the vicinity of the triple point of a Mach Stem.

Comparison of the data with the `LOAD_BLAST_ENHANCED` empirical model indicates that the use of this empirical model for height-of-burst simulations does a reasonable job of predicting maximum impulse in the Mach Stem region, but not above the triple point. Predicted times-of-arrival of the Mach Stem provide an acceptable average value, and agree well with the the measurements above the triple point. Similarly, the first peak pressures agree with the measurement above the triple point, but under predicted in the Mach Stem region. Agreement above the triple point of arrival times and initial peak pressures is to be expected, as these results are identical to the ConWep. Overall, this engineering model provides a very cost effective approximation of the loads experienced by a structure subjected to a height-of-burst generated Mach Stem.

Comparison of the data with the MM-ALE model results indicates the 2D axisymmetric MM-ALE model over estimates the impulse both below and above the trip point by about 39%, which is a significant difference. Simulations using a reduced 3D MM-ALE model and the available mapping feature provide a much improved agreement with the Kisters and Kuder maximum impulse data. The improved 3D model results are attributed to pressure clearing in the vicinity of the vertical gauge array, which is not possible with the 2D axisymmetric model.

## 9 Acknowledgements

The author acknowledges the excellent experimental work performed by Drs. Kristler and Kuder of EMI, upon which the present comparisons are based. The help and advice of Mr. Todd Slavik and Dr. Nicolas Aquelet of Livermore Software Technology Corporation on the present work, and numerous past activities, is much appreciated.

## 10 Reference

Kisters, T., and J. Kuder, 2012, *Experimental Characterization of a Near-Field HOB-Detonation*, Proceedings of the 22nd International MABS Symposium, Bourges, France

UFC 3-340-02 *Unified Facilities Criteria (UFC) Structures to Resist the Effects of Accidental Explosions*, United States Department of Defense, December 2008.

Aquelet, N., and M. Souli, 2008, *2D to 3D ALE Mapping*, LS-DYNA International Conference, Dearborn, MI

<http://www.dynalook.com/international-conf-2008/FluidStructure-3.pdf>

Lapoujade, V., N. Van Dorsselaer, S. Kevorkian, and K.Cheval, 2010, *A Study of Mapping Technique for Air Blast Modeling*, LS-DYNA International Conference, Dearborn, MI

<http://www.dynalook.com/international-conf-2010/BlastImpact-1-3.pdf>

CAB (Close-in Air Blast) Version 1.10.1, "Distribution authorized to U.S. Government agencies and their contractors; Critical Technology, December 1997. Other requests for this program shall be referred to the USAE Engineer Research & Development Center, CEERD-GS-S, 3909 Halls Ferry Road, Vicksburg, Mississippi 39180."

ConWep (Conventional Weapons) Version 2.1.08, "Distribution authorized to U.S. Government agencies and their contractors; Critical Technology, December 1997. Other requests for this program

shall be referred to the USAE Engineer Research & Development Center, CEERD-GS-S, 3909 Halls Ferry Road, Vicksburg, Mississippi 39180”

Unified Facilities Criteria (UFC) “Structures to Resist the Effects of Accidental Explosions,” UFC 3-340-02 5 December 2008

[http://www.wbdg.org/ccb/DOD/UFC/ufc\\_3\\_340\\_02\\_pdf.pdf](http://www.wbdg.org/ccb/DOD/UFC/ufc_3_340_02_pdf.pdf)

## 11 Appendix - LOAD\_BLAST\_ENHANCED Input Parameters

```
*LOAD_BLAST_ENHANCED
$  BID   WGT   XB0   YB0   ZB0  TB0  IUNIT  BLAST
   1, 1000.0,  0.0,  &HOB,  0.0, 0.0,   8,   4
$    CFM           CFL   CFT   CFP

$   GNID   GVID
   223000,   100
$
$                               Node for Ground Definition
*Node
223000,  0.0, 0.0, 0.0, 0, 0
$
$                               Vector for Ground Definition
*Define_Vector
$  VID   XT   YT   ZT   XH   YH   ZH  CID
   100, 0.0, 0.0, 0.0,  0.0, 1.0, 0.0
```

## 12 Appendix – CAB Graphical User Interface Inputs

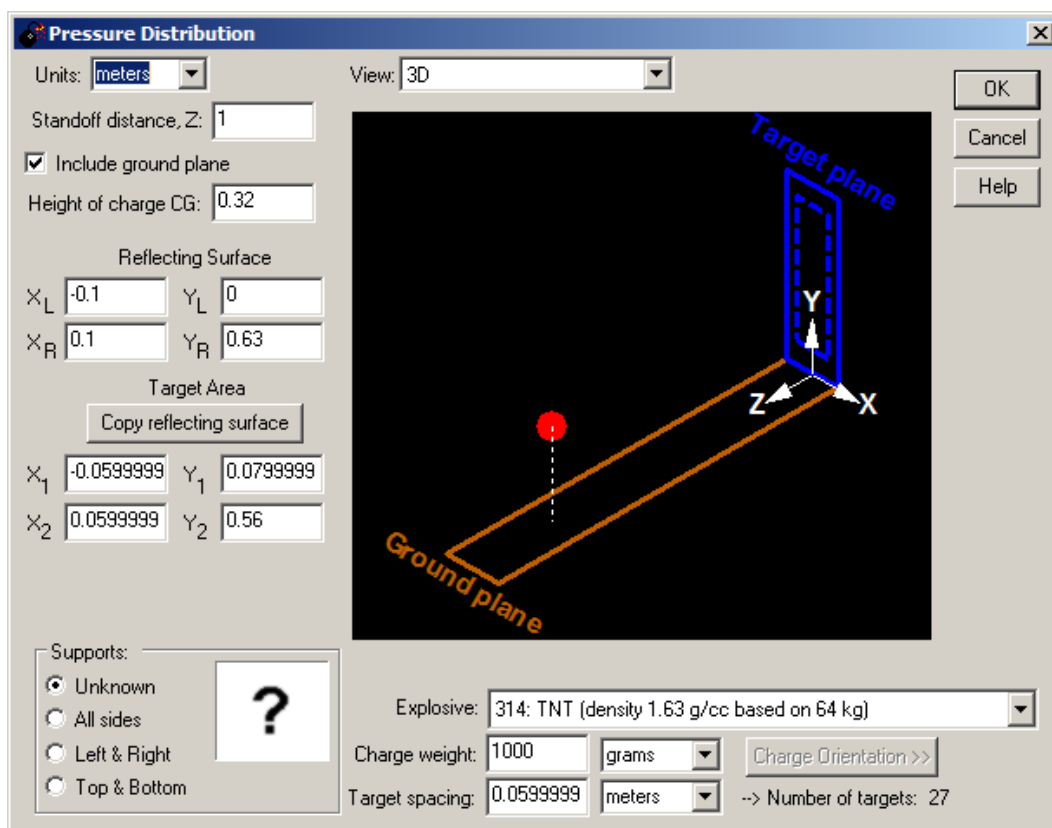


Figure 31 Cab inputs for simulation of Kisters and Kuder height-of-burst experiment.

### 13 Appendix – Air and TNT Input Parameters

```

$ Properties for Air - units grams-millimeters-milliseconds
$
*MAT_NULL
$ MID RO PC MU TEROD CEROD YM PR
 10, 1.29e-6, 0.0, 0.0, 0.0, 0.0
$
*EOS_Linear_Polynomial
$ EOSID C0 C1 C2 C3 C4 C5 C6
$ 10 , -0.1, 0.0, 0.0, 0.0, 0.4, 0.4, 0.0
 10 , -0.0, 0.0, 0.0, 0.0, 0.4, 0.4, 0.0
$ e0 v0
 0.25, 1.0
$

$ Properties TNT units grams-millimeters-milliseconds
*MAT_HIGH_EXPLOSIVE_BURN
$ MID RO D PCJ BETA
 20, 1.631E-3, 0.67174E4, 0.18503E5, 0.0
$
$ TNT
*EOS_JWL
$ EOSID A1 A2 A3 A4 A5
 20 , 490.07e5, 56.868e5, 0.82426e5, 0.00093e5
$ R1 R2 R3 R4 R5
 40.713, 9.6754, 2.4335, 0.15564
$ AL1 AL2 AL3 AL4 AL5
 0.00, 11.468
$ BL1 BL2 BL3 BL4 BL5
 1098.0, -6.5011
$ RL1 RL2 RL3 RL4 RL5
 15.614, 2.1593
$ C OMEGA E V0
 0.0071e5, 0.30270, 0.06656e5, 1.0
$

```

### 14 Appendix – 1D-to-2D-to-3D Mapping: Execution and Keywords

The 1D to 2D mapping commands were explained in detail in the body of the text. The continuing mapping commands for the 2D to 3D mapping are quite similar.

The three LS-DYNA execution lines would proceed as follows:

1D Simulation – LS-DYNA.exe		map=1D-1mm	i=1D-1mm-
Model.k			
2D Simulation – LS-DYNA.exe	map1=2D-2mm	map=1D-1mm	i=2D-2mm-
Model.k			
3D Simulation – LS-DYNA.exe		map=2D-2mm	i=3D-8mm-
Model.k			

The same INITIAL\_ALE\_MAPPING and SET\_MULTI-MATERIAL\_GROUP\_LIST keyword inputs would be used in the 3D input file as were used in the 2D input; refer back to the explanation in the body of the text.

For the 2D to 3D mapping, the DEFINE\_VECTOR ID specified on the INITIAL\_ALE\_MAPPING keyword is important as this vector defines how the 2D axis of symmetry is to be mapped onto the 3D mesh. For the present 3D model, refer back to Figure 23, the Y-axis in the 3D model is the same as the axis of symmetry in the 2D model. Thus the following vector definition is used:

```
*DEFINE_VECTOR
$ VID   XT   YT   ZT   XH   YH   ZH   CID
    222, 0.0, 0.0, 0.0, 0.0, 1.0, 0.0
```